Identification of Biomarkers for Deep Brain Stimulation using Electroencephalography and Diffusion Weighted Imaging

Mariana Baginha da Lança Falcão
Instituto Superior Técnico, University of Lisbon

November 2018

Abstract

Deep brain stimulation (DBS) has been successfully applied to reduce motor symptoms in patients with Parkinson's disease (PD), by modulating pathological brain networks activity via delivery of high-frequency electrical pulses. Despite the successful identification of anatomical targets and the emergence of innovative electrode technologies for application in PD, setting optimal stimulation parameters is still an elemental procedure, based on manual tuning and visual analysis of the patient's symptomology. The master project presented here aims to understand some of the changes in both brain structure and function as a consequence of PD, to improve its diagnostic and treatment. In order to find differences in the brain structure, connectivity matrices were computed from diffusion-weighted images, and their predictive power was determined. Classification accuracy of 0.79 was reached with a simple diaglinear discriminant analysis, using a binary connectivity matrix. Optimizing the classification hyperparameters in the future may lead to the development of a new diagnostic tool for PD, or even of a new tool for suitability evaluation of patients for DBS implantation. For understanding the brain function changes with DBS, resting state electroencephalography (rs-EEG) signals were recorded in 4 PD patients before and after their DBS implantation surgery, and then with different stimulation patterns. The variation of synchronized oscillations in the beta frequency range (beta burst) was investigated. Compared with a healthy control group, pre-surgical rs-EEGs show longer beta bursts, and all post-surgical rs-EEGs show a reduction in the duration of the bursts. No significant variability between the different electrical stimulation patterns was found.

Keywords: Parkinson's Disease, Deep Brain Stimulation, Diffusion Weighted Imaging, Connectivity Matrix, Electroencephalography, Beta Burst

Introduction

Parkinson's Disease (PD) is the second most common age-related neurodegenerative disorder (following Alzheimer's disease), and it is estimated to affect seven million to ten million people worldwide. This disorder has a strong prevalence over the elderly population, but it can begin in earlier stages of life, such as the age of 50. It is mainly characterized by a loss of motor learning and movement control, and the most prevalent symptoms include bradykinesia, resting tremor, rigidity, and postural instability [3]. Many research teams have tried to find discriminant differences between PD patients and healthy subjects. Inside the field of diffusion-weighted imaging (DWI), several groups have used microstructural measurements from diffusion tensor imaging (DTI). Clement et al. compared differences in Fractional Anisotropy (FA) and Mean Diffusivity (MD) in a review paper gathering results from 39 different groups [3]. Some of the variations reported were the decrease of FA in the substantia nigra (SN), temporal and cingulate cortices and the increase of MD in the SN, putamen, globus pallidus, and olfactory, temporal and cingulate cortices. However, the significance of these results was not always good, especially at the subcortical level. Possible reasons for the low significance were the small size of the subcortical regions, combined with the difficulty to do a proper segmentation, as well as the variability of demographics, DTI acquisition parameters and anatomical segmentations between studies. Other groups have looked at the brain as a network and have compared nodal graph measures, such as strength, clustering coefficient, and centrality [4, 5]. Once again, there were

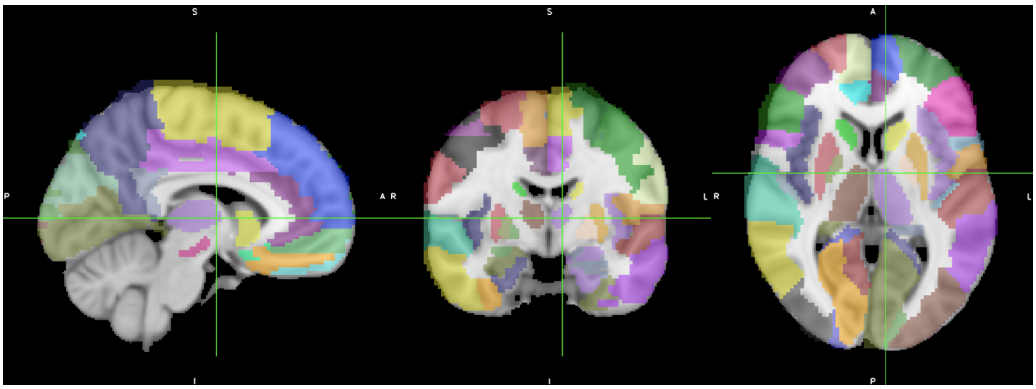

Figure 1: Final atlas used to segment my datasets. This atlas resulted from merging the subcortical atlas of Xiao [1] with the cortical structures of the AAL atlas [2].

no consistent differences between PD patients and healthy subjects, and, as a result, a more in-depth analysis should be done. Moreover, turning to a more automated way to find discriminant features of PD and building predictive models could make the diagnostic of the disease much more efficient.

When the dopaminergic medication stops working in PD patients, the alternative is to use the Deep Brain Stimulation (DBS) therapy, where an electric current is applied in specific subcortical regions of the brain, such as the Substantia Nigra (SN), causing the reduction of the motor symptoms of PD. Up to this day, stimulation parameters of DSB are chosen by trial and error, based on changes observed by the doctors. This biased approach limits the therapeutic potential of DBS and leads to reduced improvement in both motor and non-motor symptoms, as well as to the appearance of side-effects [6]. As a result, research has leaned towards finding an accurate way to set optimal stimulation parameters for each PD patient treated with DBS. Several research groups have so far observed an increased synchronization in the beta frequency range (13 - 30H z), when measuring the brain electrical activity of Parkinsonian patients using Local Field Potentials (LFP) in the subthalamic nucleus (STN) [7, 8]. Others have already tried to see if this synchronization is reduced with dopaminergic medication [9] or with DBS [10, 11, 12]. However, due to its invasiveness, LFP recordings are rarely done in healthy individuals, causing a drawback in the comparison of PD signals with a control population. Therefore, finding these beta frequency oscillations in a non-invasive technique, such as the electroencephalography (EEG), could facilitate the comparison with a control population, and thus improve the future optimization of DBS.

Methods

Diffusion Weighted Imaging

The Dataset. T1 and DWI data were downloaded from the Parkinson's Progression Markers Initiative (PPMI) database [13], and two groups were built: the *De Novo Parkinsonian Patients* group (PD group), integrating 50 PD patients with 3 MRI acquisitions over time (150), and the control group, containing 38 healthy individuals with 2 MRI acquisitions over time (76). Inclusion criteria for PD patients was a recent diagnostic (two years or less before the first acquisition) and no administration of dopaminergic medications; inclusion criteria for controls was the absence of PD and no first-degree blood relative with PD. Additionally, MRI scans were acquired in the Centre Hospitalier Universitaire Vaudois (CHUV), in Lausanne, Switzerland, from 4 Parkinsonian patients who were going to be implanted with a DBS device.

Pre-processing of DWI signals. Anatomical (T1) and DWI brain structures were cropped. Each T1 image was co-registered to the corresponding DWI images. The single fiber response was estimated from the Tax Response function estimation algorithm. T1 white matter mask was extracted. The Constrained Spherical Deconvolution algorithm computed the fiber orientation distribution function of every voxel, and, then, the probabilistic tractography algorithm predicted brain tracts. In a parallel analysis, the diffusion tensor was computed from the DWI, and the FA and MD were obtained. In order to produce a region-wise connectivity matrix from the tractography, a segmentation atlas was defined (Figure 1). This atlas was the result of merging two different atlases, the Automated Anatomical Labeling (AAL) atlas [2], for cortical regions, and an additional subcortical at-

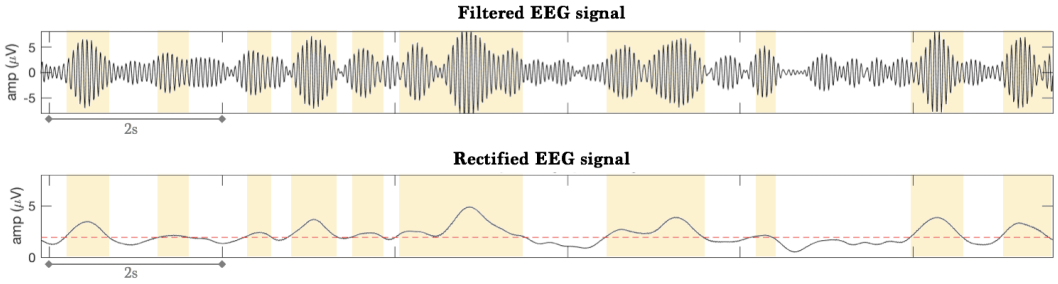

Figure 2: Pipeline for beta burst detection. The pre-processed EEG is first filtered around the frequency of interest, and then it is rectified. Later, an amplitude threshold is defined from the 75th percentile of the EEG signal, and the bursts are detected when the rectified signal reaches the defined threshold.

las, created by Xiao and colleagues [1]. The last atlas was built based on Parkinsonian MRI data, so it is expected to register the subcortical regions nicely. In order to register the final atlas in the patients' DWI space, the following sequence of steps was computed: the T1 was non-linearly registered in the MNI space, and a transformation was obtained; the inverse of that transformation was used to bring the atlas into the T1 space; and, finally, the transformation from the T1 to the DWI space was used to transfer the atlas into the diffusion space. From the tractography and the atlas registration in the DWI space, four different connectivity matrices (CM) were computed: a binary CM, a streamline CM (with the number of streamlines in each connection), and two CMs injected with microstructural information (FA and MD). The streamline CM was normalized by the total number of voxels of every two connected regions. Due to the small nature of the subcortical structures, all connections with more than one streamline were considered.

Connectivity matrix. Each of the four connectivity matrices was reshaped into a single row vector (reciprocal connections were not repeated) and packed together to obtain a matrix with the number of subjects as rows (226), and the number of connections as columns. Leave one (subject) Out Infinite Feature Selection [14] was performed to each of the four large matrices, to extract the most discriminant features. Then, simple classifiers were built: linear discriminant analysis, diaglinear discriminant analysis, diagquadratic discriminant analysis, k-nearest neighbors and decision trees. For every classifier type, a Leave One (subject) Out cross-validation was performed. The accuracy, receiver operating characteristic (ROC) curve, sensitivity, specificity, area under the curve (AUC) were calculated for every classifier.

Reproducibility analysis. Three measures of reproducibility were calculated for the control group, in order to verify the stability of the best connections found: the intraclass correlation coefficient (ICC), the within-subject coefficient of variation (CV-intra) and the between-subject coefficient of variation (CV-inter). Reproducibility can be evaluated from the ICC values calculated, with the following guidelines: poor reproducibility (ICC $<$ 0.40); fair reproducibility (0.40 $\leq$ ICC $<$ 0.60); good reproducibility (0.60 $\leq$ ICC $<$ 0.75); excellent reproducibility (ICC $\geq$ 0.75) [15]. For biological measurements with MRI, CV-intra $\leq$ 10% and CV-inter $<$ 15% are considered as acceptable [16, 17].

Correlation with UPDRS. From the best classifier obtained, the posterior probability and the distance to the hyperplane were computed. Both measures were correlated with individual UPDRS scores or with summed UPDRS per parts. The Pearson correlation coefficient was calculated, and the highest correlation values were analyzed.

Graph Measures. Local and global graph measures were computed for each connectivity matrix [4]. Every Local graph measure was used separately for classification, the global measures were used together, and finally, all measures were put together for classification. Fisher-Score was used to select the best features for every case. The classification pipeline for this section is identical as the one from the previous section, but the graph measures were only calculated for the best connectivity matrix type obtained from before, and from the best classification type.

Electroencephalography

The Dataset. For the control group, 16 healthy subjects with one eyes-closed resting state EEG (rs-EEG) were selected from the AGE-ility dataset (age = 33.1 $\pm$ 1.2) [18]. For the PD dataset, data from the 4 PD patients recorded in the CHUV was used (age = 60.8 $\pm$ 7.8). These patients were go-

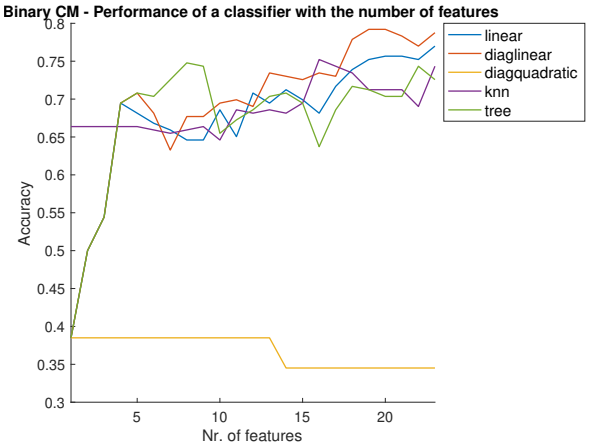

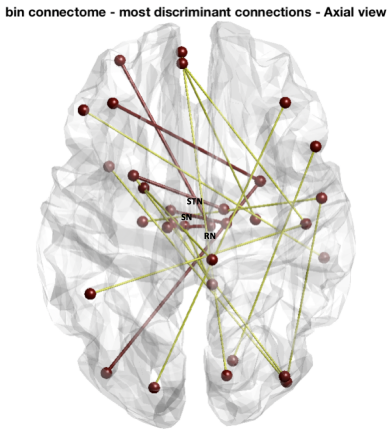

Figure 3: ***left.*** *Accuracy of classification between Control and PD groups, using five different classifiers (linear, diaglinear, diagquadratic, k-nearest neighbors and decision trees. Most classifiers have similar performances when increasing the number of connections used. The diagquadratic classifier is the only one not being able to fit the data for this amount of features, which might mean that the data is better to split with a first-order polynomial.* ***right.*** *20 most discriminative connections of the binary connectivity matrix: axial, sagittal and coronal views.*

ing to be implanted with a Deep Brain Stimulation (DBS) device, so it was possible to record their eyes closed rs-EEG both before and after the implantation. Each patient recorded one rs-EEG pre-surgery, one or more rs-EEG post-surgery OFF stimulation, and two or more rs-EEG post-surgery ON stimulation (with different stimulation patterns per recording).

Pre-processing of the EEG signals. For each recording, channels which were not recording brain activity were removed. A bandpass filter with cutoff frequencies 1Hz and 40 Hz was applied to each channel, and each signal was downsampled to a sampling frequency of 128Hz. Noisy channels were interpolated by the adjacent channels; the new signal was re-referenced, and, finally, local artifacts were manually removed.

Frequency analysis. The EEG signal was split in windows of 2s. The mean FFT spectrum and the standard deviation (SD) were computed for all windows in each channel and, then, the average spectrum was visualized. For the frequency band between 16 Hz and 22 Hz, the mean and SD previously computed were averaged and the z-score was computed.

Beta burst analysis. Every EEG signal was filtered around the maximum frequency peak (bandpass filter of $f_P - 3$ - $f_P + 3$ Hz) and then rectified around a 0.4 s window. The beta bursts were determined from the time points at which the DC corrected, smoothed, rectified and filtered beta signal exceeded a given threshold amplitude along time (Figure 2). An amplitude threshold was defined as the 75th percentile of the rectified signal [12, 9]. The duration of a beta burst was determined as the time between exceeding and falling below the threshold, and its amplitude was determined as the maximum signal amplitude during that time. For the PD patients, due to the high number of recordings that were performed, the applied threshold was set as the average of the threshold amplitudes for every recording. In order to avoid spurious beta bursts, bursts with duration values three standard deviations higher or lower than the average duration were discarded. The same eliminatory procedure was done to discard spurious burst amplitudes.

Results

Diffusion Weighted Imaging

Connectivity matrix. Figure 3 shows the classification accuracy of multiple classifiers using a different number of features for the binary CM. To compare the remaining classification performances, we used the diaglinear classifier containing 20 features, as they bring the best classification performance. The best 20 connections of the binary CM (Figure 3) appeared in more than 98% of the time Leave one (subject) out feature selections. Interesting regions which found to be discriminant were frontal regions, occipital regions, STN, substantia nigra, putamen, thalamus, and red nucleus. Accuracy, sensitivity, specificity, and AUC results are shown in Table 1. Between the binary CM, streamlines CM, FA CM and MD CM, the one with

20 features/ diaglinear classifier	Class Accuracy	Sensitivity	Specificity	AUC
Binary CM	0.79	0.64	0.92	0.88
(Chance level)	0.50	0.32	0.65	0.47
Streamlines CM	0.73	0.59	0.81	0.79
(Chance level)	0.5	0.32	0.65	0.48
Streamlines CM w/ binary features	0.72	0.57	0.84	0.81
CM + FA	0.79	0.67	0.86	0.86
(Chance level)	0.47	0.30	0.63	0.45
CM + FA w/ binary features	0.76	0.61	0.87	0.83
CM + MD	0.80	0.67	0.9	0.89
(Chance level)	0.44	0.26	0.60	0.40
CM + MD w/ binary features	0.76	0.61	0.87	0.82
Strength	0.67	0.52	0.73	0.65
(Chance level)	0.65	0.38	0.67	0.51
Betweenness Centrality	0.65	0.47	0.71	0.64
(Chance level)	0.62	0.37	0.67	0.55
Eigenvalue Centrality	0.69	0.54	0.75	0.67
(Chance level)	0.62	0.37	0.67	0.55
Clustering coefficient	0.57	0.26	0.65	0.51
(Chance level)	0.66	0	0.66	0.32
Local Efficiency	0.66	0	0.66	0.46
(Chance level)	0.65	0	0.66	0.38
Global measures	0.66	0	0.66	0.025
(Chance level)	0.66	0	0.66	0.06
20 Best features overall graph measures	0.67	0.51	0.75	0.69
(Chance level)	0.63	0.39	0.67	0.58

Table 1: Table with classification accuracy, sensitivity, specificity and area under the curve (AUC) values obtained for each classifier. Chance level classifications were also performed.

the best performance was the MD CM (class. accuracy = 0.80; sens. = 0.67; spec. = 0.9; AUC = 0.89). However, it has almost the same performance as the binary CM (class. accuracy = 0.79; sens. = 0.64; spec. = 0.92; AUC = 0.88) and the FA CM (class. accuracy = 0.79; sens. = 0.67; spec. = 0.86; AUC = 0.86). Therefore, injecting of the MD and the FA does not seem to add much information to the binary CM. On the other hand, adding the proportional amount of streamlines between connections diminishes the performance of the classifier (class. accuracy = 0.73; sens. = 0.59; spec. = 0.81; AUC = 0.79). From Table 1 we can also see that the classification performance is considerably above the chance level classification in all cases (chance level accuracy values are 0.50 for the binary CM, 0.47 for the FA CM, 0.44 for the MD CM and 0.50 for the streamlines CM), so the classification results were data driven. Finally, there was no improvement on the classification when using the best 20 features of the binary CM in the other connectivity matrices.

In order to validate the model, the DWI data from 3 PD patients, gathered in CHUV, was used as a validation set. Using the binary CM prediction model, all 3 subjects were classified to be Parkinsonian patients (100% classification accuracy).

Reproducibility Analysis. The average ICC value (0.57 ± 0.08) was closer to the ICC values of subcortical connections (0.57 ± 0.07) than from the cortical ICC values (0.71 ± 0.09). The maximum and minimum values of our best features (0.74 and 0.44 respectively) were in the range of ICC values of cortical and subcortical connections (0.94 - 0.41 and 0.74 - 0.39 respectively). Regarding the stability analysis, 60% of connections were considered to have fair reproducibility, and 40% was considered to have good reproducibility. No connections had poor reproducibilities. Regarding the coefficients of variation, high variability values were observed for the CV-intra (from 46.3% to 438.9%) and the CV-inter (from 59.2% to 456.8%). Therefore, none of the connections are considered stable, according to the previous guidelines. However, these CV values were not defined for single connections, but instead for more global measures, which have more stable behavior. Even for the cortical connections (the most stable, due to the size of the cortical structures), only 1.3% of the CV-intra values and 0.3% with CV-inter values were considered as reproducible. This values are very low and do not seem to represent well the data.

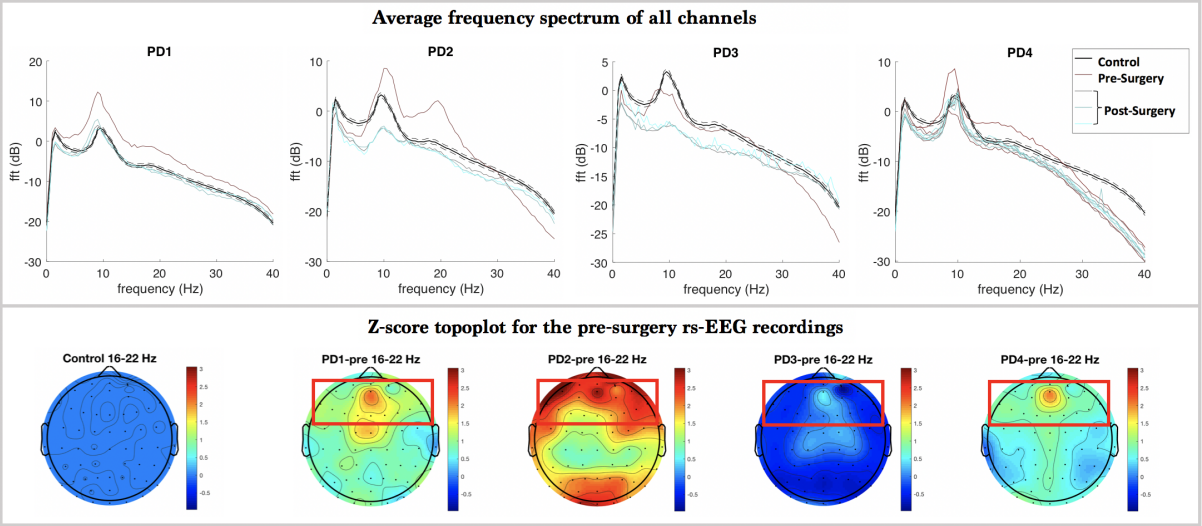

Figure 4: ***top.*** *Differences in the average frequency spectrum between the healthy population and patients 1 to 4 (from right to left), without dopaminergic medication and before and after DBS implantation surgery and stimulation.* ***bottom.*** *Differences in the average z-score between the same two groups, for the frequency band of 16 - 22 Hz. For patients 1, 2 and 4, differences are mostly located at the frontal region of the scalp. Patient 3 shows a smaller variation from the healthy population.*

Correlation with UPDRS. The best correlations found for the posterior probability were with the resting tremor amplitude score of the right upper limb (Pearson coeff. $= 0.220$, p-val $= 0.007$) and the toe-tapping score of the right foot (Pearson coeff. $= 0.215$, p-val $= 0.008$); and for the distance to the classification hyperplane were with the toe-tapping score of the right foot (Pearson coefficient $= 0.245$, p-val $= 0.005$) and the leg agility score of the right leg (Pearson coefficient $= 0.256$, p-val $= 0.002$).

Graph measures. Results are shown in Table 1 Comparing with the classification performances obtained with the connections, classifying with the graph measures brings out a lower performance (the highest class accuracy achieved was 0.69, 0.10 units lower than the binary connectivity classification - 0.79; and with an area under the curve of 0.67, more than 0.20 units lower than the AUC of the binary CM classifier). The chance level performance values were very similar from the ones obtained in the real classification.

Merging different analysis A final analysis was to observe if using both types of measures would improve the prediction model. For this case, the best 20 features of the binary connectivity matrix and the best 20 features overall graph measures were selected and used to predict PD. The obtained classification performance (class. accuracy = 0.75, sensitivity = 0.60, specificity = 0.87, AUC = 0.83) was lower than the classification performances calculated using only the connectivity measures (Table 1).

Electroencephalography

Frequency analysis. Figure 4 shows a comparison between the average frequency spectrums of each patient before and after DBS implantation surgery and the average frequency spectrum from the healthy groups. An additional standard error of the control group is presented in the plots. Pre-surgically, an amplitude increase around the beta frequencies is observed for patients 1, 2 and 4. From the topoplot it is possible to observe the average z-score of the pre-surgical rs-EEG signals for the frequency range 16 - 22 Hz, discriminated for each channel. Except for patient number 3, all the other patients show a high variance amplitude (z-score$>$1.7, p-val$=$0.05 [19]) in frontal channels. Post-surgically, a general decrease in FFT amplitude was observed in every recording from patients 1, 2 and 4. For these patients, every post-surgical acquisitions had a spectrum with similar amplitudes as from the healthy spectrum. For patient 3, the pre-surgical spectrum had a similar amplitude than the healthy population, whereas all post-surgical spectrums showed a lower amplitude signal, mainly in the alpha and beta ranges. Finally, one interesting observation is that, although each post-surgical recording had different types of stimulation (OFF and ON with different stimulation electrodes), every frequency spectrum appeared to be

very identical, and no significant changes were verified in order to be able to discriminate the different types of stimulation.

Beta Burst analysis The first measure computed was the categorization of the beta burst duration in 9 time windows of 100 ms, starting from 100 ms. The results presented in Figure 5.A. show that, in general, the pre-surgical rs-EEG signal had a smaller number of short bursts (between 100 ms and 400 ms) and a slightly higher number of long bursts (between 800 ms and 1 s). When inserting the DBS electrode, both with and without stimulation, the number of short bursts increased whereas the number of long bursts decreased. Additionally, in the post-surgical EEG recordings, differences between OFF and ON stimulation did not appear to be as significant as the differences from pre-surgical EEG recordings. For the average burst duration measures (Figure 5.B.), once again, pre-surgery recordings (without any medication or stimulation) showed longer bursts comparing with the controls as well as the post-surgery recordings (both OFF and ON stimulation), and there were no significant differences between OFF and ON stimulation recordings. Regarding the percentage of time each signal spent as a burst (Figure 5.C.), signals with higher beta burst duration were the pre-surgery data, and there was almost no differentiation between the different post-surgery recordings. Regarding the amplitude of the beta burst (Figure 5.D.), we can see higher amplitude values in the pre-surgical signals, mainly for longer bursts, as well as reduced amplitude of the longer bursts in the post-surgical recordings.

Discussion

Using diffusion to reconstruct the connections between brain structures, we can find connections which discriminative between healthy and PD brains. Hitherto, using a simple diaglinear classifier and only 20 connections from the more than 4000 connections existing in a segmented brain, it was possible to achieve a classification performance of 80%. Perhaps if in the future, the classification parameters were optimized, we could improve the discriminative power of this classification.

From the results obtained for all connectivity matrices, the sensitivity of the classification was always considerably lower than the specificity of the classification. This interesting result led us to the conclusion that the connectivity features used are successfully discarding the existence of the disease in healthy subjects (true negatives), but have more difficulty in diagnosing Parkinsonian patients with PD (true positives). Nevertheless, the sensitivity value is a good value, since it can diagnose more than 50% of the Patients. Additionally, when we used our validation set to measure the performance of our best classifier (DWI data of 3 PD patients), there was an accuracy of 100%. One explanation for the low sensitivity values might be related to the different stages of PD along the disease time. A patient with a more advanced stage of disease will, in theory, have more significant structural differences when compared with a patient in a very early stage. As a result, patients in earlier stages might be misclassified. Nonetheless, when trying to correlate the clinical score of the patients with their classification performance, we did not obtain a very high correlation. Of course that we are correlating a biased score with an objective classifier, and that one single clinical score per recording does not reflect the real stage of development of the disease. In fact, the UPDRS clinical score of each patient can be influenced by fatigue, medication, emotional factors, among others. Therefore, one clinical score might not reflect the stage of disease of the patient entirely. Using graph measures did not predict PD. A possible explanation is that graph measures generalize too much and that the discriminant structural information about PD is provided by the circuitry between several different structures of the brain. Richiardi and colleagues [20] had arrived at the same conclusion with functional MRI.

In order to increase the classification performance, several improvements could be considered from the beginning of the analysis. One possibility could be the implementation of multishell acquisitions for the DWI, known to increase the precision of the tractography [21]. Other improvements could pass by improving the brain segmentation. The built atlas has interesting features and is fast to register, but, due to the low contrast of the scanned images, it is not able to be correctly registered in the brain structure. One solution could be to use higher resolution segmentations (such as the *FreeSurfer* toolbox [22]), but higher segmentation accuracy is more time-consuming. Next, there is the choice of the tractography algorithm. By choosing to use a probabilistic tractography, and considering a connection when there is at least one streamline between regions, we are jeopardizing the integrity of the information in the connectivity matrices by adding spurious connections to it. Nonetheless, there was the need to guarantee connections to

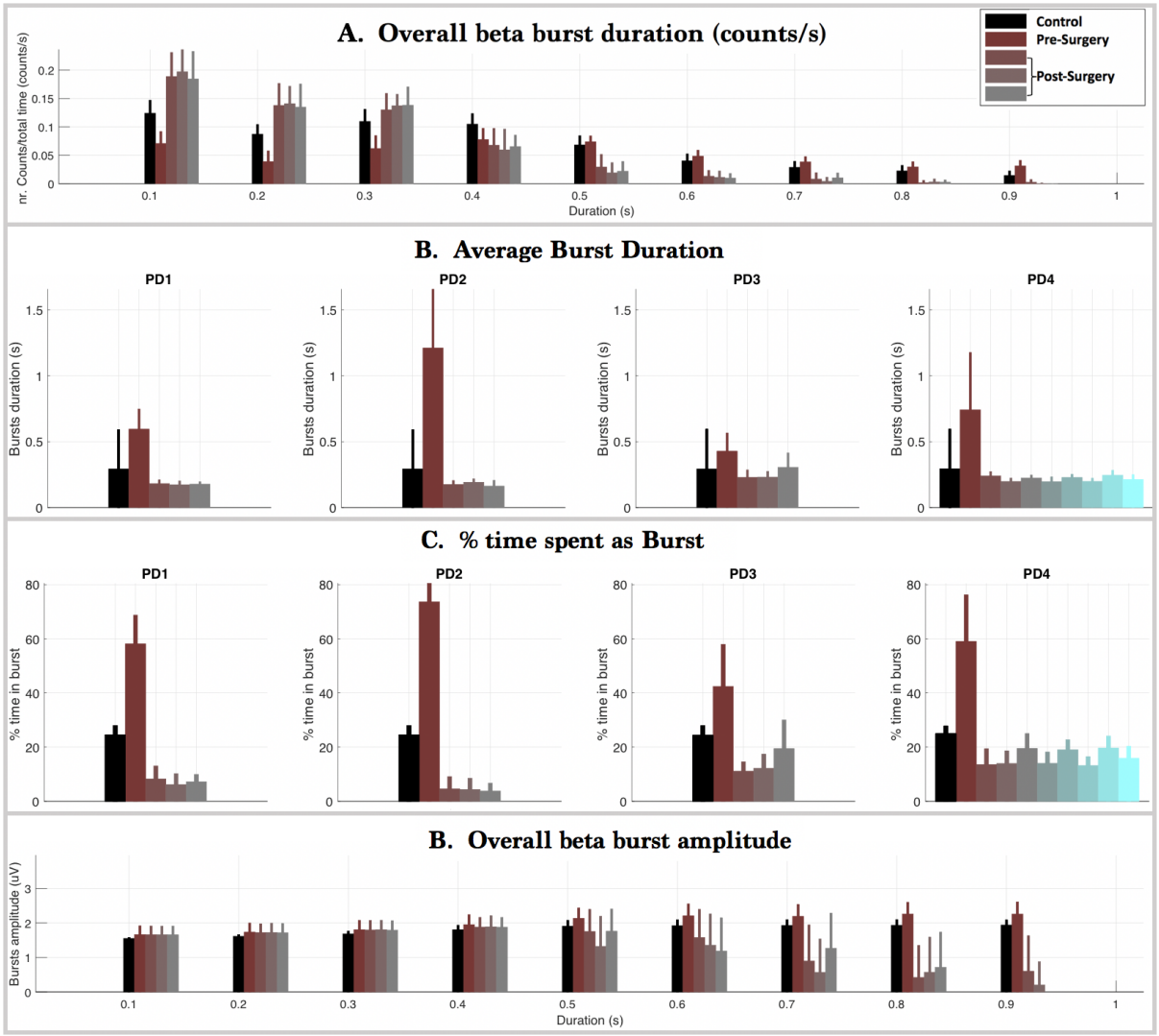

Figure 5: ***A.*** *Example of categorization of the beta bursts duration in 9 time windows of 100 ms (i.e., the first window is between 100 ms and 200 ms, and so on). For all four patients, beta bursts tend to have a longer duration for the pre-surgery stage of the recordings, and, after DBS implantation, the beta bursts are shorter in duration. In none of the cases, the PD signal comes closer to the healthy behavior, but the post-surgery acquisition appears to be the closest to it. The various post-surgery acquisitions do not show very significative differences.* ***B.*** *Average burst duration in each rs-EEG recording for patients PD1 to PD4 (from left to right). Beta bursts from the pre-implantation surgery recordings have a longer average duration time, but they also have a high duration variability. Similarly, all post-surgical recordings (either OFF and ON stimulation) have a shorter average burst duration. These average durations are integrated into the distribution of the healthy beta burst duration. Nevertheless, the control variability is also high, in comparison with the post-surgical variability.* ***C.*** *Percentage of time each rs-EEG signal recoding spent in burst mode, for patients PD1 to PD4 (from left to right). For the pre-implantation recordings, compared with the controls, the signal is above the beta burst threshold for an extended period in all patients. After surgery, for all patients, the percentage of time the signal is in burst mode is reduced and becomes even smaller than what was observed for the controls.* ***D.*** *Average burst amplitude for the categorized beta bursts along nine time windows of 100 ms. For short bursts, there is no variability between any rs-EEG recordings. For long bursts, average amplitudes between controls and pre-surgery recordings are similar and are in general reduced for the post-implantation recordings (both ON and OFF stimulation). Additionally, there seems to be higher variability in the amplitude values for longer bursts.*

small subcortical structures, which due to their size and location, are unlikely to be determined in tractography. Therefore, a better balance between guaranteeing subcortical connections and reducing spurious connections could be analyzed further in detail. The threshold choice might also be one of the reasons why the use of a streamline connectivity matrix has a lower performance in the classification. Finally, although infinite feature selection seems to be a suitable feature selection type (since it considers the connections between regions as a graph and not as independent features), there might also exist better feature selection tools.

Regarding the Electroencephalography analysis, there are three major discussion topics. The first comparison regards the rs-EEG signals of pre-surgery Parkinsonian patients and healthy controls. A general observation for all patients was the tendency to have a smaller number of short bursts and a larger number of long bursts in PD patient. This variance in burst duration led to an overall increase of the time each electrical signal is spent in burst mode. Regarding the amplitude of the bursts, the differences are less noticeable, but it is possible to observe a slight increase in the burst amplitude for the PD patients for the longer bursts. The increase both in the amplitude and in the duration of the beta bursts agrees with what other research groups had already found in previous studies using LFP's [7, 9, 10, 12].

The second interesting observation is between the two previous groups of recordings (control and PD pre-surgery) and post-implantation surgery patients. For the post-surgery acquisitions, in general, the duration of bursts becomes shorter and with lower amplitude. These results had also been verified before by other research teams [10, 11, 12] using LFP's, but, from the best of my knowledge, it is the first time that it has ever been reported using rs-EEG, and comparing with a healthy control group. Additionally, it appears sometimes that the duration of beta bursts is even shorter than the one reported by the healthy subjects. That could mean that the brain is not being able to regulate its electrical activity properly in order to reach a healthy pattern. Another explanation could be the differences in brain signals associated with young age of the healthy subjects (33.1 ± 1.2) [23].

Finally, there is the analysis of all the post-implantation surgery recordings. Although each acquisition performed post-surgically used different stimulation parameters (OFF and ON with different electrodes), none of them showed significant differenced in the recordings. One possible explanation could be the surgery effect suffered by the patients, since the time between the post-surgery recordings and the electrode implantation surgery was too short (one to two days). Indeed, the electrode implantation is an invasive procedure and foments the appearance of temporary lesions in the brain, which consequently induce temporary effects, such as the reduction motor symptoms of PD [24]. This lesioning effect might be the only phenomena we observe in the recordings, and, therefore, no influence in stimulation will be able to change the state of the brain. Another possible explanation is the short time between each rs-EEG recordings. Previous studies found that turning the stimulation ON or OFF does not change immediately the features of PD [25]. In our case, due to several factors, including the weakness of the patient post-surgically, recordings were shrunken into periods of around 5 min and started 2 to 3 minutes after the beginning of the stimulation pattern. As a result, there was no time to adapt to each of the types of stimulation, and there could have been an accumulated effect of the different stimulations overall recordings. One final explanation is the possibility that the changes between the different stimulations and the OFF stimulation were too small to be detected by the beta burst changes in the EEG, and that maybe the beta burst analysis is not a suitable biomarker measure to report these changes.

In all three comparisons, it was harder to find differences in beta burst amplitude than in duration. This difficulty might come from the fact that the EEG registers a smoother and noisier signal in comparison to the LFP's, and therefore the amplitude of the beta bursts might not be recorded as easily. The low amplitude variability might explain why amplitude differences in the beta range between PD patients and healthy subjects were rarely reported before.

This rs-EEG analysis could be improved with a statistical analysis, to understand better how significant the differences between different brain states of PD are, when applying DBS and when comparing with a healthy population. The statistical analysis was not performed due to the reduced sample size in this part of the project. Therefore, an increased sample size (not only for the patients but also for the controls) could give increase the statistical power of these results, and thus increasing our conclusions regarding the possible use of EEG to differentiate stages of Parkinson.

Conclusion

There exists the possibility to predict Parkinson's disease from diffusion-weighted imaging. So far, only advanced stages of PD (with motor scores) were studied, but, perhaps by improving the prediction power, it would be possible even to detect PD in earlier stages of the disease. Additionally, electroencephalography could help to optimize the DBS parameters, but only in a chronic stage of the implantation.

References

[1] Yiming Xiao, Vladimir Fonov, M. Mallar Chakravarty, Silvain Beriault, Fahd Al Subaie, Abbas Sadikot, G. Bruce Pike, Gilles Bertrand, and D. Louis Collins. A dataset of multi-contrast population-averaged brain mri atlases of a parkinson's disease cohort. *Data in Brief*, 12:370–379, 2017.

[2] N. Tzourio-Mazoyer, B. Landeau, D. Papathanassiou, F. Crivello, O. Etard, N. Delcroix, B. Mazoyer, and M. Joliot. Automated anatomical labeling of activations in spm using a macroscopic anatomical parcellation of the mni mri single-subject brain. *NeuroImage*, 15:273–289, 2002.

[3] C. A. Clement, S. Pinto, A. Eusebio, and O. Coulon. Diffusion tensor imaging in parkinson's disease: Review and meta-analysis. *NeuroImage: Clinical*, 16:98–110, 2017.

[4] S. Nigro, R. Riccelli, L.Passamonti, G. Arabia, M. Morelli, R. Nistico, F. Novellino, M. Salsone, G. Barbagallo, and A. Quattrone. Characterizing structural neural networks in de novo parkinson disease patients using diffusion tensor imaging. *Human Brain Mapping*, 37:4500–4510, 2016.

[5] G. Barbagallo, M.E. Caligiuri, G. Arabia, A. Cherubini, A. Lupo, R. Nistico, M. Morelli, G. L. Cascini, D. Galea, and A. Quattrone. Structural connectivity differences in motor network between tremor-dominant and nontremor parkinson's disease. *Human Brain Mapping*, 38:4716–4729, 2017.

[6] A. M. Lozano and N. Lipsman. Probing and regulating dysfunctional circuits using deep brain stimulation. *Neuron*, 77:406–424, 2013.

[7] Chiung Chu Chen, Yi Ting Hsu, Hsiao Lung Chan, Shang Ming Chiou, Po Hsun Tu, Shih Tseng Lee, Chon Haw Tsai, Chin Song Lu, and Peter Brown. Complexity of subthalamic 13-35hz oscillatory activity directly correlates with clinical impairment in patients with parkinson's disease. *Experimental Neurology*, 224:234–240, 2010.

[8] Doris D. Wang, Coralie de Hemptinne, Svjetlana Miocinovic, Salman E. Qasim, Andrew M. Miller, Jill L. Ostrem, Nicholas B. Galifianakis, Marta San Luciano, and Philip A. Starr. Subthalamic local field potentials in parkinson's disease and isolated dystonia: An evaluation of potential biomarkers. *Neurobiology of Disease*, 89:213–222, 2016.

[9] Gerd Tinkhauser, Alek Pogosyan, Huiling Tan, Damian M. Herz, Andrea A. Kühn, and Peter Brown. Beta burst dynamics in parkinson's disease off and on dopaminergic medication. *Brain*, 140:2968–2981, 2017.

[10] A. A. Kühn, F. Kempf, C. Brucke, L. Gaynor Doyle, I. Martinez-Torres, A. Pogosyan, T. Trottenberg, A. Kupsch, G.-H. Schneider, M. I. Hariz, W. Vandenberghe, B. Nuttin, and P. Brown. High-frequency stimulation of the subthalamic nucleus suppresses oscillatory activity in patients with parkinson's disease in parallel with improvement in motor performance. *Journal of Neuroscience*, 28:6165–6173, 2008.

[11] Simon Little, Alex Pogosyan, Spencer Neal, Baltazar Zavala, Ludvic Zrinzo, Marwan Hariz, Thomas Foltynie, Patricia Limousin, Keyoumars Ashkan, James FitzGerald, Alexander L. Green, Tipu Z. Aziz, and Peter Brown. Adaptive deep brain stimulation in advanced parkinson disease. *Annals of Neurology*, 74:449–457, 2013.

[12] Gerd Tinkhauser, Alek Pogosyan, Huiling Tan, Damian M. Herz, Andrea A. Kühn, and Peter Brown. Beta burst dynamics in parkinson's disease off and on dopaminergic medication. *Brain*, 140:2968–2981, 2017.

[13] Parkinson's progression markers initiative (ppmi). Available at: www.ppmi-info.org. [Accessed 12 Set. 2018].

[14] G. Roffo, S. Melzi, and M. Cristani. Infinite feature selection. In *2015 IEEE International Conference on Computer Vision (ICCV)*, pages 4202–4210, 2015.

[15] Domenic V. Cicchetti. Guidelines, criteria, and rules of thumb for evaluating normed and standardized assessment instruments in psychology. *Psychological Assessment*, 6:284–290, 1994.

[16] Stefano Marenco, Robert Rawlings, Gustavo K. Rohde, Alan S. Barnett, Robyn A. Honea, Carlo Pierpaoli, and Daniel R. Weinberger. Regional distribution of measurement error in diffusion tensor imaging. *Psychiatry Research: Neuroimaging*, 147:69–78, 2006.

[17] E. Heiervang, T.E.J. Behrens, C.E. Mackay, M.D. Robson, and H. Johansen-Berg. Between session reproducibility and between subject variability of diffusion mr and tractography measures. *NeuroImage*, 33:867–877, 2006.

[18] F. Karayanidis, M.C. Keuken, S.A. Wong, J.L. Rennie, G. de Hollander, P.S. Cooper, W.R. Fulham, R. Lenroot, M.W. Parsons, N. Philips, P.T. Michie, and B.U Forstmann. The age-ility project (phase 1): Structural and functional imaging and electrophysiological data repository. *Neuroimage*, 2015.

[19] z-score table. Available at: http://www.z-table.com/. [Accessed 12 Set. 2018].

[20] Jonas Richiardi, Sophie Achard, Edward Bullmore, and Dimitri Van De Ville. Classifying connectivity graphs using graph and vertex attributes. *2011 International Workshop on Pattern Recognition in NeuroImaging*, pages 978–0–7695–4399–4/11, 2011.

[21] Daan Christiaens, Marco Reisert, Thijs Dhollander, Stefan Sunaert, Paul Suetens, and Frederik Maes. Global tractography of multi-shell diffusion-weighted imaging data using a multi-tissue model. *NeuroImage*, 123:89–101, 2015.

[22] FreeSurfer. Freesurfer. Available at: https://surfer.nmr.mgh.harvard.edu/. [Accessed 12 Sep. 2018].

[23] Gennady G. Knyazev, Nina V. Volf, and Ludmila V. Belousova. Age-related differences in electroencephalogram connectivity and network topology. *Neurobiology of Aging*, 36:1849–1859, 2015.

[24] Jorge Guridi and Andres M. Lozano. A brief history of pallidotomy. *Neurosurgery*, 41:1169–1183, 1997.

[25] P. Temperli, J. Ghika, J.-G. Villemure, P.R. Burkhard, J. Bogousslavsky, and F.J.G. Vingerhoets. How do parkinsonian signs return after discontinuation of subthalamic dbs? *Neurology*, 60:78–81, 2003.